arXiv:1209.6445v1 [q-bio.NC] 28 Sep 2012

A Balance Between Competitive and Cooperative Ion Channels Regulates Neuronal Excitability

Alessio Franci[1,#], Guillaume Drion[1,2,#], Laurent Massotte[2], Vincent Seutin[2] & Rodolphe Sepulchre[1,*]
[1]Department of Electrical Engineering and Computer Science and GIGA Research, University of Liège, Liège, Belgium.
[2]Neurophysiology Unit, GIGA Neurosciences, University of Liège, Liège, Belgium.
#These authors contributed equally to this work.
* E-mail: R.Sepulchre@ulg.ac.be

Abstract

We use the qualitative insight of a planar neuronal phase portrait to detect an excitability switch in arbitrary conductance-based models from a simple mathematical condition. The condition expresses a balance between ion channels that provide a negative feedback at resting potential (competitive channels) and those that provide a positive feedback at resting potential (cooperative channels). Geometrically, the condition imposes a transcritical bifurcation that rules the switch of excitability through the variation of a single physiological parameter. The application of this algorithm to six different published conductance based models always finds the transcritical bifurcation in a physiological parameter range, which suggests that the mathematical predictions have a physiological relevance and that a same regulatory mechanism is potentially involved in the excitability and signaling of many neurons. An experiment on midbrain dopaminergic neurons illustrates the predictive power of the balance condition by highlighting a role of cooperative L-type calcium channels in regulating the neuron firing pattern.

Author summary

Understanding the changing electrophysiological signatures of neurons in different physiological and pharmacological conditions is a central focus of experimental electrophysiology because a key component of cell signaling in the nervous system. Computational modeling may assist experimentalists in this quest by identifying core mechanisms and suggesting pharmacological targets from a mathematical analysis of the model. But a successful interplay between experiments and mathematical predictions requires new analysis tools adapted to the complexity of high-dimensional computational models nowadays available. We use bifurcation theory to propose a mathematical condition that can detect an important switch of neuronal excitability in arbitrary conductance-based neuronal models and we illustrate its physiological relevance in six published state-of-the art models of different neurons.

Introduction

Detailed computational conductance-based models have long demonstrated their ability to faithfully reproduce the variety of electrophysiological signatures that can be recorded from a same neuron in varying physiological or pharmacological conditions. But the predictive value of a computational model is limited unless its analysis sheds light on the core mechanisms at play behind a computer simulation. Because conductance-based models are nonlinear dynamical models, their analysis often requires a drastic reduction of dimension. The reduced model is amenable to the geometric methods of dynamical systems theory, but the mathematical insight is often gained at the expense of physiological interpretability; hence the need for methodological tools that can relate mathematical predictions of low-dimensional models to physiological predictions in detailed conductance based models.

In recent work [1], we used phase plane analysis and dynamical bifurcation theory to characterize in *reduced-order* neurodynamics models a switch of excitability that is consistent with many physiological observations. More precisely, a transcritical bifurcation governed by a single parameter was shown to organize a switch from competitive excitability, extensively studied in most models inspired from the Hodgkin-Huxley model, to cooperative excitability, whose distinct electrophysiological signature is shared by most bursting neurons.

The main contribution of the present paper is to show that this transcritical bifurcation, and the associated excitability switch, exist in a number of *high-dimensional* conductance-based models and that the resulting mathematical predictions have a strong physiological relevance. More precisely, we provide an algorithm to trace the transcritical bifurcation in arbitrary conductance-based models. Although purely mathematical in nature, the detection of the transcritical bifurcation is based on an ansatz that leads to a remarkably simple physiological interpretation: the switch of excitability is determined by a balance between competitive (those providing a negative feedback) and cooperative (those providing a positive feedback) ion channels at the resting potential. Because this simple tuning rule can take many different physiological forms, it is potentially shared by very different neurons. We apply the algorithm to detailed conductance-based models of six neurons known to exhibit drastic changes in their electrophysiological signatures depending on environmental conditions: the squid giant axon [2], the dopaminergic neuron [3], the thalamic relay neuron [4], the thalamic reticular neuron [5], the aplysia R15 model [6], and the cerebellar granular cell [7]. In each case, the algorithm identifies a the transcritical bifurcation that occurs in a physiological range of parameters and its prediction correlates with experimental observations.

In the case of dopaminergic neurons, our mathematical analysis suggests that the heterogeneity of L-type calcium channels across populations has little effect on the pacemaking but a strong effect on bursting. We validate this prediction via experimental results that are in strong agreement with the model prediction.

After defining a novel classification of ion channels based on their competitive or cooperative nature, we briefly review the planar model presented in [1] and how its transcritical bifurcation qualitatively captures the switch between competitive and cooperative excitability. As a generalization of this low-dimensional case, we mathematically construct the same bifurcation in generic conductance based models and derive the balance condition determining the cooperative or competitive nature of the model. This construction and its electrophysiological predictions are firstly illustrated on the squid giant axon. An algorithm for generic conductance-based models is subsequently derived and different models analysed. In particular, we revisit, using a TC neuron model as an insightful example, how neuronal signalling can rely on the dynamic regulation of the balancing between competitive and cooperative ion channels. Finally, we illustrate our results in an experiment on midbrain dopaminergic neurons.

Results

Competitive and cooperative ion channels

Conductance-based models of neurons describe the dynamic interaction between the membrane potential V and - possibly many - gating variables that control the ionic flow through the membrane. The gating of ion channels occurs on many different timescales. However, gating timescales can be grouped in three families, according to their influence on neuronal excitablity [8]:

(i) **Fast gating variables**: These variables have a time-constant in the millisecond range. They generate the rapid regenerative upstroke of an action potential. Prominent representatives of this family are the activation gating variables of fast voltage-gated sodium channels ($\mathrm{Na_V}1.1$ to $\mathrm{Na_V}1.9$).

(ii) **(Slow) Recovery gating variables**: These variables have a time constant 5 to 10 times larger than fast gating variables. They influence the spike initiation, downstroke, and the afterspike period. They are the key players of neuronal excitability. Prominent representatives of this family are the activation gating variables of delayed rectifier potassium channels ($\mathrm{K_V}1.1$ to $\mathrm{K_V}1.3$, $\mathrm{K_V}1.5$ to $\mathrm{K_V}1.8$, $\mathrm{K_V}2.1$, $\mathrm{K_V}2.2$, $\mathrm{K_V}3.1$, $\mathrm{K_V}3.2$, $\mathrm{K_V}7.1$ to $\mathrm{K_V}7.5$, $\mathrm{K_V}10.1$) and the activation gating variables of all calcium channels ($\mathrm{Ca_V}1.\mathrm{x}$, $\mathrm{Ca_V}2.\mathrm{x}$, $\mathrm{Ca_V}3.\mathrm{x}$).

(iii) **(Ultra-Slow) Adaptation variables**: These variables gate too slowly to be strongly activated by single action potentials. They modulate neuronal excitability only over periods of many action potentials. Prominent representative of this family are the inactivation gating variables of transient calcium channels

(Ca_V2.x, Ca_V3.x). Adaptation variables might also include non gating variables. For instance, the intracellular calcium concentration $[Ca^{2+}]_{in}$, which modulates the conductance of calcium-regulated channels.

In view of their importance for neuronal excitability, we focus only on recovery gating variables to classify ion channels: when the recovery variable opposes a variation of the membrane potential by negative feedback, we term the associated channel a competitive ion channel. When the recovery variable instead enhances a voltage variation by positive feedback, the associated ion channel is termed cooperative. Ion channels that do not possess a recovery gating variable are neither competitive nor cooperative and are called neutral. Neutral ion channels solely regulate the "quantity" of excitability without affecting its "quality".

Table 1 shows a classification of many known ion channels according to this criterion. Not surprisingly, potassium channels are the main representatives of competitive ion channels. By increasing the total outward current, their activation induces a negative feedback on membrane voltage variations that is responsible for neuron repolarization. On the other hand, physiologically described calcium channels are all cooperative. Their activation induces an increase of the total post-spike inward current, in contrast to potassium channels. This is the source, for instance, of afterdepolarization potentials (ADP). Interestingly, sodium channels can be either competitive, cooperative, or neutral according to their fast transient, resurgent, or persistent behavior, respectively.

Ion Channel	**Gating Kinetics**	**Classification**
Sodium Channels		
Transient	FA, SI - Negative feedback via SI	Competitive
Persistent	FA - No slow gating variable	Neutral
Resurgent	SA, USI - Positive feedback via SA	Cooperative
Calcium Channels		
L-type	SA - Positive feedback via SA	Cooperative
T-type	SA, USI - Positive feedback via SA	Cooperative
N, P/Q, R-type	SA, USI - Positive feedback via SA	Cooperative
Potassium Channels		
Delayed Rectifiers	SA - Negative feedback via SA	Competitive
KCNQ	USA - No slow gating variable	Neutral
eag/erg	USA - No slow gating variable	Neutral
A-type	FA, SI - Positive feedback via SI	Cooperative
BK	SA - Negative feedback via SA	Competitive
HCN	SA - Negative feedback via SA	Competitive

FA: fast activation, FI: fast inactivation, SA: slow activation, SI: slow inactivation, USA: utraslow activation, USI: ultraslow inactivation

Table 1. Classification of ion channels according to their gating kinetics. Activation and inactivation variables are distributed in three groups: fast, (slow) recovery, and (ultra-slow) adaptation. Recovery variables are defined as competitive (resp. cooperative) if they induce a negative (resp. positive) feedback on membrane potential variations. An ion channel that posses a competitive variable is called "competitive channel", and similarly for cooperative channels. Channels that do not posses a recovery variable are called "neutral channels". This classification might change for a given channel for some channel subtypes.

It is important to observe that the competitive (resp. cooperative) nature of channels is not solely linked to the outward (resp. inward) nature of the current. For instance, transient sodium channels are competitive, because their recovery variable inactivates an inward current, inducing a negative-feedback on membrane potential variations. Similarly, potassium channels can be cooperative when their slow inactivation massively decreases the outward current, like in the case of A-type potassium channels.

Although elementary, the classification above seems novel. It is motivated by the central message of this paper, that the balance between cooperative and competitive ion channels in a given neuron determines it neuronal excitability type.

Competitive and cooperative excitability in planar models

Planar models - that only consist of two state variables - have been instrumental to study excitability since the early days of neurodynamics [9, 10]. Empirical planar reductions of conductance based models only retain the (fast) voltage variable V and one (slow) recovery gating variable n. Fast gating variables are set to steady-state (i.e. their fast variation is approximated as instantaneous), adaptation variables are treated as slowly varying parameters, and the sole recovery variable aggregates all recovery variables, expressing each of them as a (curve-fitted) state function of n.

Based on such empirical reduction of the Hodgkin-Huxley model augmented with a calcium channel [11], our recent study [1] explores the neuronal excitability of the planar model

$$\dot{V} = V - \frac{V^3}{3} - n^2 + I_{app} \tag{1a}$$

$$\dot{n} = \varepsilon(n_\infty(V - V_0) + n_0 - n) \tag{1b}$$

whose phase portraits are reproduced in Fig. 1 for two distinct values of the parameter n_0 (an indirect image of the calcium conductance in the high-dimensional model). The parameter $\varepsilon > 0$ is an image of the time-scale separation between V and n. The function $n_\infty(\cdot)$ has the standard sigmoid shape of conductance-based models and V_0 is the half-activation potential. The phase portrait in Fig. 1 left is the qualitative phase portrait of FitzHugh-Nagumo model. It is associated to a reversible and sudden switch from rest to firing and has extensively been studied, with finer distinctions between excitability types I (SNIC), II (Hopf), III (no bifurcation), depending on the mathematical nature of the underlying bifurcation. See [12, Section 3.4.4],[13],[14, Section 7.1.3] and reference therein.

The phase portrait in Fig. 1 right is in sharp contrast in that the electrophysiological response to a current input exhibits spike latency, plateau oscillations, and after depolarization potential (ADP). This specific signature, experimentally observed in many families of neurons, is fundamentally associated to the bistability illustrated in the phase portrait: namely, the robust coexistence of two stable attractors (a hyperpolarized resting potential and a limit cycle of periodic action potentials) and a saddle-separatrix that sharply separates their basins of attraction. The time evolution shown in the top figure is a consequence of this phase portrait and cannot be observed in FitzHugh-Nagumo like phase portraits. In that sense, it is an electrophysiological signature of competitive excitability. A finer distinction between excitability types IV (saddle-homoclinic) and V (saddle-saddle) is discussed in [1] depending on the nature of the bifurcations that surround the bistable range.

A simple mathematical distinction between the two phase portraits shown in Fig. 1 is drawn from the Jacobian linearization of the model at the stable resting point $(\bar{V}, \bar{n})$:

$$J = \left. \begin{pmatrix} \dfrac{\partial \dot{V}}{\partial V} & \dfrac{\partial \dot{V}}{\partial n} \\ & \\ \dfrac{\partial \dot{n}}{\partial V} & \dfrac{\partial \dot{n}}{\partial n} \end{pmatrix} \right|_{(\bar{V},\bar{n})} = \begin{pmatrix} * & -2\bar{n} \\ \underbrace{\varepsilon \dfrac{\partial n_\infty}{\partial V}(\bar{V} - V_0)}_{>0} & -\varepsilon \end{pmatrix} .$$

The product of the partial derivatives $\frac{\partial \dot{V}}{\partial n}\frac{\partial \dot{n}}{\partial V} = -2\bar{n}\,\varepsilon \frac{\partial n_\infty}{\partial V}(\bar{V} - V_0)$ is negative on the left phase portrait (small variations of the recovery variable provide negative feedback on the voltage) whereas it is positive on the right (small variations of the recovery variable provide positive feedback on the voltage). This difference is schematized in the block diagrams of Fig. 2. The reader familiar with mathematical biology will recognize the positive feedback interconnection as the basic circuit motif for multi-stationary regimes [15].

The planar model (1) can smoothly switch from competitive to cooperative excitability, with a transition occurring for $\bar{n} = 0$, or, in algebraic terms,

$$\frac{\partial \dot{V}}{\partial n}\frac{\partial n_\infty}{\partial V} = 0 \tag{2}$$

A convenient way to algorithmically track this excitability switch is to use bifurcation analysis and to impose that the critical condition (2) coincides with a bifurcation of the model, which imposes the additional algebraic condition

$$\det J = 0. \tag{3}$$

Simultaneously imposing (2) and (3) implies

$$\frac{\partial \dot{V}}{\partial V} = 0, \tag{4}$$

which, in geometrical terms, corresponds to the transcritical bifurcation obtained for $I_{app} = \frac{2}{3}$ and illustrated in Fig. 3.

The theory of bifurcation unfolding is further exploited in [1] in order to classify all excitability types associated to the planar model in Fig. 1. This analysis results in five different types of excitability obtained by varying the two parameters (V_0, n_0) around the singular phase portrait of Fig. 3, center. The parameter n_0 acts in particular as the sole regulator of the balance between cooperative and competitive excitability by shifting the n-nullcline up and down: a positive n_0 corresponds to a phase portrait as in Fig. 3 left, whereas the phase portrait of Fig. 3 right is obtained for sufficiently negative n_0. The associated parameter chart is reproduced in Figure 4. It contains the five types of excitability discussed above.

Our main contribution in the present paper is to show that the diagram in Fig. 4 is not an artifact of planar reduction but captures excitability transitions that can algorithmically be tracked in conductance-based models of arbitrary dimension.

Competitive and cooperative excitability in conductance based models

We start by grouping gating variables of a given conductance-based model according to their time scales. The family $\mathcal{G}_F = \{m_{Na,f},\ m_{Na,p},\ m_{K,A}, \ldots\}$ collects fast gating variables. The gating variable $x^f \in [0,1]$ denotes a generic member of this family. Similarly, the family $\mathcal{G}_R = \{h_{Na,f},\ m_{K,DR},\ m_{Ca,L}, \ldots\}$ collects recovery gating variables x^r, whereas $\mathcal{G}_A = \{h_{Ca,T},\ h_{Na,R},\ m_{K,M}, \ldots\}$ collects adaptation variables x^a. For a given ion channel type i, the standard notation m_i (resp. h_i) is adopted for the activation (resp. inactivation) gating variable of the associated ionic current I_i. With these notations, a general neuron conductance-based model reads

$$C_m \dot{V} = -\sum_i \bar{g}_i m_i^{a_i} h_i^{b_i} (V - E_i) + I_{app}, \tag{5a}$$

$$\tau_{x^f}(V)\dot{x}^f = (x^f_\infty(V) - x^f), \tag{5b}$$

$$\tau_{x^r}(V)\dot{x}^r = (x^r_\infty(V) - x^r), \tag{5c}$$

$$\tau_{x^a}(V)\dot{x}^a = (x^a_\infty(V) - x^a), \tag{5d}$$

where the sum in (5a) is over all ion channels in the model, and (5b),(5c),(5d) hold for all the associated fast, recovery, and adaptation variables, respectively. The activation (resp. inactivation) functions x^f_∞, x^r_∞ are strictly monotone increasing (resp. decreasing) sigmoids. In the forthcoming analysis, all adaptation variables are treated as constant parameter, that is their slow evolution is neglected.

We will detect a switch from competitive to cooperative excitability by mimicking the two-dimensional algorithm of the previous section. We first impose the bifurcation condition $\det J = 0$, where J denotes the Jacobian of the subsystem (5a),(5b),(5c). The algebraic condition writes

$$\det J_f + \sum_{x^r} \frac{\partial \dot{V}}{\partial x^r} \frac{\partial x^r_\infty}{\partial V} = 0 \tag{6}$$

where J_f denotes the Jacobian of the fast subsystem (5a),(5b) and the sum is over all recovery variables. The particular form of equation (6) is a direct consequence of the specific structure of conductance-based models, that is, parallel interconnection of two-dimensional feedback loops involving the voltage dynamics (5a) and one of the gating variable dynamics (5b),(5c).

As for the planar model (1), we track the switch between competitive and cooperative excitability by imposing the high-dimensional equivalent of the balance condition (2). We therefore look for solutions of (6) satisfying the ansatz

$$\sum_{x^r} \frac{\partial \dot{V}}{\partial x^r}\frac{\partial x^r_\infty}{\partial V} = 0. \tag{7}$$

The two conditions (6),(7) now imply

$$\det J_f = 0. \tag{8}$$

We show in Supplementary Material that the corresponding bifurcation is necessarily transcritical.

The singularity (8) is the high-dimensional counterpart of the V-nullcline self-intersection in the planar model. It reflects the geometric nature of the transcritical bifurcation, that is, a robust geometrical object that exists independently of the timescale separation and persists in the singular limit of an infinite timescale separation, regardless of the system dimension. Our ansatz makes the proposed analysis completely robust against the model time constants. The time constants are only used to classify the gating variables in the three physiological groups.

We split $\mathcal{G}_R$ in the two subfamilies $\mathcal{G}_{R+}$, which contains *cooperative* recovery gating variables x^{r+}, and $\mathcal{G}_{R-}$, which contains *competitive* recovery gating variables x^{r-}. The balance condition (7) is then rewritten as

$$\underbrace{\sum_{x^{r+}} \overbrace{\left.\frac{\partial \dot{V}}{\partial x^{r+}}\frac{\partial x^{r+}_\infty}{\partial V}\right|_{TC}}^{>0}}_{\text{Cooperative gates}} \quad + \quad \underbrace{\sum_{x^{r-}} \overbrace{\left.\frac{\partial \dot{V}}{\partial x^{r-}}\frac{\partial x^{r-}_\infty}{\partial V}\right|_{TC}}^{<0}}_{\text{Competitive gates}} = 0 \tag{9}$$

to express a balance between competitive and cooperative ion channels. It is the high-dimensional counterpart of (2) and it provides a rigorous high-dimensional generalization of competitive and cooperative excitability:

Competitive excitability

The model is said to be competitive at steady state if:

$$\left.\left(\sum_{x^{r+}} \frac{\partial \dot{V}}{\partial x^{r+}}\frac{\partial x^{r+}_\infty}{\partial V} + \sum_{x^{r-}} \frac{\partial \dot{V}}{\partial x^{r-}}\frac{\partial x^{r-}_\infty}{\partial V}\right)\right|_{SS} < 0$$

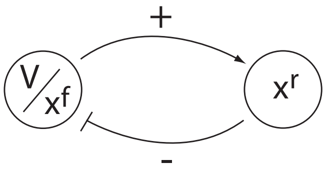

Cooperative excitability

The model is said to be cooperative at steady state if:

$$\left.\left(\sum_{x^{r+}} \frac{\partial \dot{V}}{\partial x^{r+}}\frac{\partial x^{r+}_\infty}{\partial V} + \sum_{x^{r-}} \frac{\partial \dot{V}}{\partial x^{r-}}\frac{\partial x^{r-}_\infty}{\partial V}\right)\right|_{SS} > 0$$

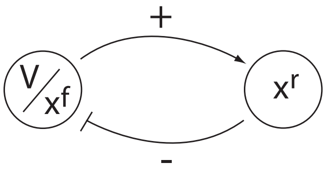

The insight provided by the planar model of the previous section predicts that the switch of excitability detected by the balance equation (9) will lead to the accompanying distinct electrophysiological signatures of Fig. 1.

Tracking excitability switches in the squid giant axon

The Hodgkin-Huxley (HH) model [2] provides a non-physiological, but historical and experimentally verified tutorial for tracking a switch of excitability in conductance based models. The model reads

$$
\begin{aligned}
C\dot{V} &= -\bar{g}_K n^4 (V - V_K) - \bar{g}_{Na} m^3 h (V - V_{Na}) - g_l (V - V_l) + I_{app}, && \text{(10a)}\\
\tau_m(V)\dot{m} &= (m_\infty(V) - m), && \text{(10b)}\\
\tau_h(V)\dot{h} &= (h_\infty(V) - h), && \text{(10c)}\\
\tau_n(V)\dot{n} &= (n_\infty(V) - n), && \text{(10d)}
\end{aligned}
$$

where m is the fast sodium channel activation while the sodium channel inactivation h and the potassium channel activation n are the (slow) recovery gating variables. We set all time constants to one, because this simplification has no effects on the algebraic conditions (7) and (8). The Jacobian of (10) reads

$$
J = \left[\begin{array}{cc|cc}
\frac{\partial \dot{V}}{\partial V} & \frac{\partial \dot{V}}{\partial m} & \frac{\partial \dot{V}}{\partial h} & \frac{\partial \dot{V}}{\partial n} \\
\frac{\partial m_\infty}{\partial V} & -1 & 0 & 0 \\
\hline
\frac{\partial h_\infty}{\partial V} & 0 & -1 & 0 \\
\frac{\partial n_\infty}{\partial V} & 0 & 0 & -1
\end{array}\right]. \tag{11}
$$

The upper-left block is the Jacobian of the fast (V, m) subsystem. Imposing the singularity condition (8) yields

$$
\left.\frac{\partial \dot{V}}{\partial V}\right|_{TC} + \left.\frac{\partial \dot{V}}{\partial m}\frac{\partial m_\infty}{\partial V}\right|_{TC} = 0, \tag{12a}
$$

while the balance equation (9) reads

$$
\left.\frac{\partial \dot{V}}{\partial n}\frac{\partial n_\infty}{\partial V}\right|_{TC} + \left.\frac{\partial \dot{V}}{\partial h}\frac{\partial h_\infty}{\partial V}\right|_{TC} = 0 \tag{13a}
$$

Note that (12) and (13) imply the bifurcation condition $\det J = 0$ in (11).

At first sight, the balance condition (13) cannot be satisfied because both sodium and potassium channels are competitive channels according to their corresponding kinetics in the model, and in agreement with our proposed classification. This is consistent with the fact that the excitability of the HH model is always competitive in physiological conditions.

However, it was long recognized [16] that potassium channels can generate an inward current at steady-state if the extracellular K^+ concentration is sufficiently large. Indeed, any change in extracellular potassium concentration induces a change in the potassium reversal potential, as expressed by the Nernst equation. This suggests to use the potassium reversal potential V_K as a bifurcation parameter in HH model in order to satisfy the balance equation

$$
\underbrace{\overbrace{\left.\frac{\partial \dot{V}}{\partial n}\frac{\partial n_\infty}{\partial V}\right|_{TC}}^{!\,>0}}_{n\text{: Cooperative gating}} + \underbrace{\overbrace{\left.\frac{\partial \dot{V}}{\partial h}\frac{\partial h_\infty}{\partial V}\right|_{TC}}^{<0}}_{h\text{: Competitive gating}} = 0 \tag{14}
$$

where potassium now acts as a cooperative gating variable provided that $V_K > V_{SS}$. Physiologically, condition (14) imposes that the potassium Nernst potential is large enough for the cooperativity of the potassium activation to balance the competitive effects of the sodium current inactivation.

The two conditions (12) and (14) can numerically be solved to determine the critical values V_K^c and V^c. The value of the applied current at the transcritical bifurcation is then determined from (10a), which gives

$$
I_{app}^c = \bar{g}_K n_\infty^4(V^c)(V^c - V_K^c) + \bar{g}_{Na} m_\infty^3(V^c) h_\infty(V^c)(V^c - V_{Na}) + g_l(V^c - V_l).
$$

The numerical bifurcation diagram in Fig. 5A confirms the transcritical bifurcation at V_K^c. That bifurcation diagram is drawn by varying V_K together with applied current I_{app}, following the affine reparametrization described in Supplementary Material. More precisely,

$$I_{app}(V_K) = I_{app}^c - \bar{g}_K n_\infty^4(V^c)(V_K - V_K^c).$$

Mathematically, this reparametrization imposes one of the defining conditions of the transcritical bifurcation. Physiologically, its effect is to keep the net current constant at steady-state V^c (*i.e.* $I_{ion}(V_K) + I_{app}(V_K) = 0$): as V_K is varied, the observed switch in the excitability type does not rely on changes in the net current across the membrane, but solely on changes in its dynamical properties.

The bifurcation diagram in Fig. 5A provides informations on the model excitability also far from the transcritical values. For highly hyperpolarized V_K, the model is purely competitive and exhibits the typical excitable behavior of the original Hodgkin-Huxley model, which corresponds to Type II excitability (see Figure 4 and [1, Figure 8]). As V_K is increased, a stable cooperative steady-state is born in a saddle-node bifurcation. At this transition, the system switches to Type V excitability, which is cooperative. Short current pulses let the system switch between the depolarized competitive steady state and the hyperpolarized cooperative stable steady state (Fig. 5B,middle). The bifurcation diagram and the phase-portrait carry the signature of Type V excitable models (Fig. 5C,D,middle) [1, Section 5]. Finally, further increase of V_K let the competitive steady state exchanges its stability with a (cooperative) saddle at the transcritical bifurcation and the system switches to Type IV excitability. The cooperative steady state coexists in this case with the spiking limit cycle attractor. Current pulses switch the systems between the two attractors (Fig. 5B,right), and the bifurcation diagram and phase portrait carry the signature of Type IV excitable models (Fig. 5C,D,right) [1, Section 5].

The same qualitative excitability switch was described by Rinzel in [10], who linked the appearance of a bistable behavior to the inward nature of potassium current at steady-state for sufficiently depolarized V_K. *In vitro* recordings of the squid giant axon with isotonic extracellular K^+ concentration show the same transition [16]. Our interpretation of this phenomenon in terms of competitive and cooperative excitability is as follows: as the potassium Nernst potential is increased, the potassium current activation gating variable becomes less and less competitive and eventually becomes cooperative. Further increases of V_K causes its cooperativity to dominate the competitivity of the sodium current inactivation, providing an overall positive feedback on the fast subsystem composed by the membrane potential and the sodium current activation, leading to cooperative excitability, as sketched in Fig. 6.

Tracking excitability switches in conductance-based models

The mathematical analysis of the previous sections follows an algorithm that allows to detect a transcritical bifurcation in generic conductance based models of arbitrary dimension and to track associated excitability switches. The steps of the algorithm are summarized in Table 2.

We now apply this algorithm to a number of published conductance-based models and show that all these models can switch between competitive and cooperative excitability through a transcritical bifurcation, as sketched in Fig. 7. Figure 7 indicates two qualitatively distinct routes from competitive to cooperative excitability: the II-V-IV route just described with Hodgkin-Huxley model (Fig. 5A) and the II-I-IV route that will be illustrated on the dopaminergic neuron model.

Dopaminergic (DA) neuron model

Model equations and parameters are taken fom [3]. This is the model that originally motivated [11].

(i) **Classification of gating variables as fast ($\mathcal{G}_F$), recovery ($\mathcal{G}_R$), and adaptation ($\mathcal{G}_A$) variables** The model includes fast sodium channels ($I_{Na,f}$), delayed-rectifier potassium channels ($I_{K,DR}$), L-type calcium channels ($I_{Ca,L}$), small conductance calcium-activated potassium (SK) channels ($I_{K,Ca}$), and calcium pumps ($I_{Ca,pump}$). We classify model variables as follows

- $\mathcal{G}_F = \{m_{Na,f}\}$
- $\mathcal{G}_{R,-} = \{h_{Na,f},\, m_{K,DR}\}$ and $\mathcal{G}_{R,+} = \{m_{Ca,L}\}$
- $\mathcal{G}_A = \{[Ca^{2+}]_{in}\}$

Algorithm for the detection of a transcritical bifurcation in generic conductance-based models and computation of the excitability switch bifurcation diagram.

(i) **Classification of gating variables as fast ($\mathcal{G}_F$), recovery ($\mathcal{G}_R$), and adaptation ($\mathcal{G}_A$) variables**

- (i-a) Following Tab. 1, group gating variables in the three groups $\mathcal{G}_F$, $\mathcal{G}_R$, and $\mathcal{G}_A$.
- (i-b) Split $\mathcal{G}_R$ in cooperative $\mathcal{G}_{R,+}$ and competitive $\mathcal{G}_{R,-}$ recovery gating variables.
- (i-c) If adaptation variables are present, set them to constant physiologically relevant values.

(ii) **Balance equation and choice of the bifurcation parameter**

- (ii-a) Select a cooperative ionic current I_{coop} and the associated cooperative recovery gating variable x^{coop}.
- (ii-b) Isolate the contribution of I_{coop} to excitability by setting to zero the conductances of all other cooperative currents, if any.
- (ii-c) Write the balance equation

$$\left.\frac{\partial \dot{V}}{\partial x^{coop}}\frac{\partial x^{coop}_{\infty}}{\partial V}\right|_{TC} = -\sum_{x^{r-}} \overbrace{\left.\frac{\partial \dot{V}}{\partial x^{r}}\frac{\partial x^{r}_{\infty}}{\partial V}\right|_{TC}}^{<0} \qquad \text{(b.eq.)}$$

- (ii-d) If I_{coop} has an adaptation variable x^a, pick it as the bifurcation parameter λ regulating the left hand side of (b.eq.), that is $\lambda = x^a$.
  If I_{coop} has no adaptation variable, pick $\lambda = \bar{g}_{coop}$.

(iii) **Singularity condition and fixed point equation**

- (iii-a) Solve (b.eq.) together with the singularity condition (8), in V and λ.
  For numerical implementation, note that the left hand side of (8) can be written as

$$\det J_f = \frac{\partial}{\partial V}\left(\left.\dot{V}\right|_{x^f = x^f_{\infty}(V)}\right)$$

- (iii-b) Plug the computed values V^c and λ^c into the fixed point equation $\dot{V}|_{TC} = 0$ to compute the value of the applied current at the transcritical bifurcation (I^c).

(iv) **Tracking of excitability switches**

Change the applied current according to the equation

$$I_{app} = I^c - \left.\frac{\partial \dot{V}}{\partial \lambda}\right|_{TC} (\lambda - \lambda^c),$$

and compute the model bifurcation diagram with V as the variable and λ as the bifurcation parameter.

Table 2

In order to unfold excitability switches, SK channel density is set to zero, since SK channels drastically attenuate DA neuron excitability by activating a strong calcium regulated potassium current [17, 18, 19]. The intracellular calcium concentration is fixed at $[Ca^{2+}]_{in} = 300\, nM$.

(ii) **Balance equation and choice of the bifurcation parameter**
The only source of cooperative excitability is provided by L-type calcium channels. The balance equation reads

$$\left.\frac{\partial \dot{V}}{\partial m_{Ca,L}} \frac{\partial m_{Ca,L,\infty}}{\partial V}\right|_{TC} = -\left.\left(\frac{\partial \dot{V}}{\partial h_{Na,f}} \frac{\partial h_{Na,f,\infty}}{\partial V} + \frac{\partial \dot{V}}{\partial m_{K,DR}} \frac{\partial m_{K,DR,\infty}}{\partial V}\right)\right|_{TC}. \tag{15}$$

We use the L-type calcium channel density $\bar{g}_{Ca,L}$ as the bifurcation parameter (*i.e.* $\lambda = \bar{g}_{Ca,L}$).

Solving Steps (iii) and (iv) of the algorithm above gives the following results[1]:

V^c	$\bar{g}^c_{Ca,L}$	I^c
-64.9167 mV	1.9473 mS/cm^2	9.5436 μA/cm^2

Note that all values are within the physiological range of the original model. In particular, the critical value $\bar{g}^c_{Ca,L}$ is roughly 1.5 times smaller than the original value one, which is consistent with the observation that the original model exhibits cooperative excitability during SK channel blockade.
The resulting bifurcation diagram is drawn in Fig. 8A. In addition to confirming the existence of a transcritical bifurcation for the computed values, it reveals the excitability switches induced by changes in L-type calcium channel density in this model: in the absence of L-type calcium channels, the model exhibits Type II excitability. As $\bar{g}_{Ca,L}$ increases, a saddle point and an unstable node emerge at a saddle-node bifurcation: the model switches to type I excitability. Further increase of $\bar{g}_{Ca,L}$ causes a transcritical bifurcation, where the stable point and the saddle exchange their stability. At this point, the stable steady-state becomes cooperative, and the model switches to cooperative Type IV excitability.

These excitability switches induce the predicted changes in the electrophysiological signatures, as illustrated in Fig. 8B. Whereas the DA neuron model instantaneously reacts to a step input of depolarizing current for $\bar{g}_{Ca,L} < \bar{g}^c_{Ca,L}$, it exhibits electrophysiological signature of cooperative excitability such as spike latency, plateau oscillations and ADP as soon as $\bar{g}_{Ca,L}$ becomes higher than $\bar{g}^c_{Ca,L}$. In addition, the model becomes strongly bistable.

Thalamic relay (RE) neuron model

Model equations and parameters are taken from [4].

(i) **Classification of gating variables as fast ($\mathcal{G}_F$), recovery ($\mathcal{G}_R$), and adaptation ($\mathcal{G}_A$) variables**
The model includes fast sodium channels $I_{Na,f}$, delayed-rectifier potassium channels $I_{K,DR}$ and T-type calcium channels $I_{Ca,T}$. We classify model variables as follows

- $\mathcal{G}_F = \{m_{Na,f}\}$
- $\mathcal{G}_{R,-} = \{h_{Na,f},\, m_{K,DR}\}$ and $\mathcal{G}_{R,+} = \{m_{Ca,T}\}$
- $\mathcal{G}_A = \{h_{Ca,T}\}$

(ii) **Balance equation and choice of the bifurcation parameter**
The only source of cooperative excitability is provided by T-type calcium channels. The associated balance equation reads

$$\left.\frac{\partial \dot{V}}{\partial m_{Ca,T}} \frac{\partial m_{Ca,T,\infty}}{\partial V}\right|_{TC} = -\left.\left(\frac{\partial \dot{V}}{\partial h_{Na,f}} \frac{\partial h_{Na,f,\infty}}{\partial V} + \frac{\partial \dot{V}}{\partial m_{K,DR}} \frac{\partial m_{K,DR,\infty}}{\partial V}\right)\right|_{TC}.$$

T-type calcium channels are dynamically regulated by a (slow) voltage-gated inactivation $h_{Ca,T}$. We use this variable as the bifurcation parameter (*i.e.* $\lambda = h_{Ca,T}$).

---

[1] In this and the subsequent tables, the reported critical values are not exact, but rounded to the last significant digit.

Solving Steps (iii) and (iv) of the algorithm above gives the following results:

V^c	$\bar{h}^c_{Ca,T}$	I^c
-61.5561 mV	0.0041	0.9074 nA/cm^2

Again, these values are in a physiological range, and the electrophysiological signatures are consistent with the excitability switches. See Fig. 9.

Thalamic reticular (RT) neuron model

Model equations and parameters are taken from [5], maximal conductances are adapted as in [11].

(i) **Classification of gating variables as fast ($\mathcal{G}_F$), recovery ($\mathcal{G}_R$), and adaptation ($\mathcal{G}_A$) variables**
The model includes fast sodium channels $I_{Na,f}$, delayed-rectifier potassium channels $I_{K,DR}$ and T-type calcium channels $I_{Ca,T}$. We classify model variables as follows

- $\mathcal{G}_F = \{m_{Na,f}\}$
- $\mathcal{G}_{R,-} = \{h_{Na,f},\, m_{K,DR}\}$ and $\mathcal{G}_{R,+} = \{m_{Ca,T}\}$
- $\mathcal{G}_A = \{h_{Ca,T}\}$

(ii) **Balance equation and choice of the bifurcation parameter**
The only source of cooperative excitability is provided T-type calcium channels. The associated balance equation has the same structure as for the thalamic relay neuron model considered above. Along the same line, we choose the T-type calcium channel inactivation $h_{Ca,T}$ as the bifurcation parameter (*i.e.* $\lambda = h_T$).

Solving Steps (iii) and (iv) of the algorithm above gives the following results:

V^c	$\bar{h}^c_{Ca,T}$	I^c
-48.8063 mV	0.1780	-0.82484 nA

As in the case of the thalamic relay neuron model, the T-type calcium channel inactivation generates a dynamical switch between competitive and cooperative excitability, significantly affecting neuron response to external inputs (Fig. 9).

Aplysia R15 neuron model

Model equations and parameters are taken from [6].

(i) **Classification of gating variables as fast ($\mathcal{G}_F$), recovery ($\mathcal{G}_R$), and adaptation ($\mathcal{G}_A$) variables**
The model includes fast sodium channels $I_{Na,f}$, delayed-rectifier potassium channels $I_{K,DR}$, slow L-type calcium channels $I_{Ca,L}$ and calcium-activated potassium channels $I_{K,Ca}$. We classify model variables as follows

- $\mathcal{G}_F = \{m_{Na,f}\}$
- $\mathcal{G}_{R,-} = \{h_{Na,f},\, m_{K,DR}\}$ and $\mathcal{G}_{R,+} = \{m_{Ca,L}\}$
- $\mathcal{G}_A = \{[Ca^{2+}]_{in}\}$

The intracellular calcium conductance is fixed at $[Ca^{2+}]_{in} = 0.09nM$.

(ii) **Balance equation and choice of the bifurcation parameter**
As in the case of DA neurons, the source of cooperative excitability is provided by L-type calcium channels, and we take their maximal conductance $\bar{g}_{Ca,L}$ as the bifurcation parameter. The associated balance equation has the same structure as for the DA neuron model considered above.

Solving Steps (iii) and (iv) of the algorithm above gives the following results:

V^c	$\bar{g}^c_{Ca,L}$	I^c
-48.0516 mV	$5.4054\ 10^{-5}$ mS/cm^2	-0.0318 μA/cm^2

Comparing the critical value $\bar{g}^c_{Ca,L}$ with the original value $\bar{g}_{Ca,L} = 4\ 10^{-3}$ mS/cm^2 shows that the bursting model proposed in [6] exhibits strong cooperative excitability. Switches of electrophysiological signatures are illustrated in Fig. 9.

Cerebellar granular cell (GC) model

Model equations and parameters are taken from [7].

(i) **Classification of gating variables as fast ($\mathcal{G}_F$), recovery ($\mathcal{G}_R$), and adaptation ($\mathcal{G}_A$) variables**
The model includes the following ion channels: fast ($I_{Na,f}$), persistent ($I_{Na,P}$) and resurgent sodium channels ($I_{Na,R}$) ; N-type calcium channels ($I_{Ca,N}$) ; delayed rectifier ($I_{K,DR)}$, A-type ($I_{K,A}$), inward rectifier ($I_{K,IR}$), calcium activated ($I_{K,Ca}$) and slow potassium channels ($I_{K,slow}$). We classify model variables as follows

- $\mathcal{G}_F = \{m_{Na,f},\, m_{Na,P}\}$
- $\mathcal{G}_{R,-} = \{h_{Na,f},\, m_{K,DR},\, m_{K,A},\, m_{K,IR}\}$ and $\mathcal{G}_{R,+} = \{m_{Na,R},\, m_{Ca,N}\}$
- $\mathcal{G}_A = \{h_{Na,R},\, h_{Ca,N},\, h_{K,A},\, m_{K,slow}\}$

We set the persistent and calcium-activated currents to zero (these two channels do not impact excitability type as anticipated by our classification and shown by D'Angelo and colleagues [7]). The inactivation of the A-type potassium current is fixed at $h_{K,A} = 0.02$ and the activation of the slow potassium current is fixed at $m_{K,slow} = 0.13$.

(ii) **Balance equation and choice of the bifurcation parameter**
The neuron model possesses two sources of cooperative excitability: resurgent sodium channels and N-type calcium channels. We apply our algorithm considering each case at a time, setting the other cooperative source to zero. As in the case of T-type calcium channels mentioned above, these two channels possess an inactivation gate, which is used as the bifurcation parameter. The associated balance equations read, respectively:

$$\left.\frac{\partial \dot{V}}{\partial m_{Na,R}} \frac{\partial m_{Na,R,\infty}}{\partial V}\right|_{TC} = -\left.\left(\frac{\partial \dot{V}}{\partial h_{Na,f}} \frac{\partial h_{Na,f,\infty}}{\partial V} + \sum_{y=DR,\,A,\,IR} \frac{\partial \dot{V}}{\partial m_{K,y}} \frac{\partial m_{K,y,\infty}}{\partial V}\right)\right|_{TC},$$

$$\left.\frac{\partial \dot{V}}{\partial m_{Ca,N}} \frac{\partial m_{Ca,N,\infty}}{\partial V}\right|_{TC} = -\left.\left(\frac{\partial \dot{V}}{\partial h_{Na,f}} \frac{\partial h_{Na,f,\infty}}{\partial V} + \sum_{y=DR,\,A,\,IR} \frac{\partial \dot{V}}{\partial m_{K,y}} \frac{\partial m_{K,y,\infty}}{\partial V}\right)\right|_{TC},$$

Solving Steps (iii) and (iv) of the algorithm above gives the following results, respectively:

V^c	$h^c_{Ca,N}$	I^c
-41.5447 mV	0.0318	5.2508 μA/cm^2

V^c	$h^c_{Na,R}$	I^c
-41.5252 mV	0.5066	5.1549 μA/cm^2

These results show that both channel densities are sufficiently high to allow dynamical excitability switches, which are due to dynamical channel (de)inactivations. Note that the N-type calcium channels contribute much more to cooperative excitability than resurgent sodium channels in this model ($h^c_{Ca,N} << h^c_{Na,R}$). The effect of N-type channel regulation on GC excitability are shown in Fig. 9. A similar switch is observed for resurgent sodium channels

Neuronal signaling through dynamic balancing of cooperative and competitive ion channels

In several of the examples analyzed in the previous section, the bifurcation parameter is a voltage-dependent (ultra-slow) adaptation gating variable of a cooperative ion channel: the T-type calcium channel inactivation $h_{Ca,T}$, the N-type calcium channel inactivation $h_{Ca,N}$, or the resurgent sodium channel inactivation $h_{Na,R}$. The physiological implication is that, in all these examples, any regulation of the resting potential acts as a regulator of the balancing between cooperative and competitive ion channels and therefore as a regulator of excitability.

We illustrate this regulation mechanism on reticular and relay cells of the thalamus, whose firing patterns have been linked to awakeness and sleep [20].

Fig. 10A illustrates that, as predicted by our bifurcation analysis, the excitability of RT cells is cooperative at hyperpolarized resting potential of -95 mV ($h_{Ca,T} \approx 1 > h^c_{Ca,T}$) whereas it is competitive at a normal resting potential of -57 mV ($h_{Ca,T} \ll h^c_{Ca,T}$).

The amount of cooperative channels that can be activated therefore depends on the resting potential. The latter can be regulated by $GABA_B$ metabotropic receptors, for instance. As a consequence, the model predicts two possible excitability patterns in response to external sensory stimuli:

(i) "Linear integration" (competitive) - With a depolarized resting potential, the competitive (Type I) excitability of the neuron causes a linear integration of external stimuli, faithfully transmitted to the cortex. In the case of the lateral geniculate nucleus, this firing mode has been suggested to support a faithful reconstruction of the visual world [21].

(ii) "Wake-up call" (cooperative) - With a hyperpolarized resting potential, the cooperative (Type IV) excitability of the neuron is associated to a burst response to external stimuli. The signal-to-noise ratio is higher during bursting, which enhances its detectability. This maximization of stimulus detection has been suggested to detect sudden changes in the environment [21]. The bursting mode is transient because of the slow inactivation of calcium channels (Fig. 10B), letting the model switch back to the linear integration competitive regime.

This prediction is consistent with the hypotheses that the transient burst could serve as a "wake-up call", switching the neuron from a silent state to a responsive state where stimuli can be transmitted to the cortex. These two firing modes correspond to the "up-state" of the thalamus, where external stimulations are detected, integrated and transmitted to the cortex. Note that the "down-state" of the thalamus, observed during slow-wave sleep and absence seizures, is associated to spontaneous synchronized burst of TC neurons. Those cellular rhythms also exhibit cooperative excitability but the synchronization of bursts involves additional population mechanisms not discussed in the present paper.

In conclusion, our analysis suggests that the complex firing patterns of the TC neuron owe much to a simple but regulated balance between competitive and cooperative channels.

DA neuron signaling and cooperative excitability

Our analysis in the previous sections predicts that the L-type calcium conductance $\bar{g}_{Ca,L}$ is a tuner of cooperative excitability in the DA neuron model [3]. Specifically, our model predicts cooperative excitability in the absence of small conductance calcium-activated potassium (SK) channels, provided that $\bar{g}_{Ca,L}$ is sufficiently large.

Physiologically, the parameter $\bar{g}_{Ca,L}$ is an image of the L-type calcium channel density. The density of these channels has been suggested to exhibit some heterogeneity among DA neuron population [22, 23, 3]. As a consequence, the type of excitability of DA neurons under the blockade of SK channels is expected to be heterogenous across a population of DA neurons.

We tested this hypothesis on DA neuron extracellular recordings from the substantia nigra pars compacta (SNc) in the presence of synaptic blockers (10 mM CNQX, 1 mM MK801, 10 mM SR95531, 1 mM sulpiride and 1 mM CGP55845, which block AMPA, NMDA, GABA$_A$, D2 and GABA$_B$ receptors, respectively) (Fig. 11). Control experiments showed that application of the synaptic blockers alone induced a small increase in firing rate which was stable for at least one hour [3]. The application of Apamin 300 nM, a SK channel blocker, has mixed effects on DA neuron excitability: whereas it barely affect firing rate and pattern in some neurons (Fig. 11A, left), it strongly increases irregularities and/or induces spontaneous bursting in others (Fig. 11A, right). The application of a L-type calcium channel blocker (Nifedipine 20 μM) reversed the effect of SK channel blockade on DA neuron signaling, regularizing the firing pattern in all neurons (Fig. 11B). This suggests that L-type calcium channels play an important role in the SK channel blockade induced irregularities and bursting of DA cells *in vitro*.

These results show that the L-type calcium channel density has a critical impact on the spiking pattern and therefore on the excitability type of DA neurons, although it barely affects the pacemaking activity. If the L-type calcium channel density is low, the total ionic current provides a negative feedback on membrane potential variations (Fig. 11C, top), and the neuron fires in tonic single spike, a signature of competitive excitability. By contrast, if the L-type calcium channel density is high, the positive feedback provided by these channels is dominant (Fig. 11C, bottom), and the neuron exhibits burst firing, a signature of cooperative excitability. The experiment confirms that in this latter situation only the application of the L-type calcium channel blocker nifedipine can have a critical impact on the firing pattern by inhibiting the positive feedback provided by calcium channels, therefore generating a switch from cooperative to competitive excitability.

The role of L-type calcium channels in DA firing patterns has been controversial to date [22, 23], mainly because the heterogeneity of L-type channels does not seem to affect the pacemaking activity of DA neurons. We explained in previous work [3] that this robustness relies on the collaboration of L-type calcium channels and sodium channels in generating the pacemaking activity. In this sense, calcium and sodium channels are redundant. In contrast, our analysis suggests that calcium channels and sodium channels have a different, and in fact antagonistic, contributions to the quality of neuronal excitability, a difference that is unravelled only by the blockade of SK channels. SK channels activate indeed a strong calcium regulated after-spike potassium current that masks any excitability switch by regularising the spiking pattern to a robust pacemaking activity [17, 18, 19]. To sum up, the L-type calcium channels strongly affect excitability and bursting as cooperative channels, whereas they can be substituted by sodium channels for pacemaking.

Blockade of L-type calcium channels has recently been suggested as a potential guard against neurodegeneration [24, 25]: it would protect the neuron against a calcium inflow associated to pacemaking, a source of metabolic stress favoring neurodegeneration [26, 27]. Results in this section suggest however that this blockade would at the same time significantly affects the neuron excitability even if it does not affect the pacemaking activity.

Discussion

A simple and robust balance equation identifies a transcritical bifurcation in arbitrary conductance based models

Motivated by a geometric analysis of a qualitative phase portrait, we have proposed an algorithm that can detect a transcritical bifurcation in arbitrary conductance based models. Owing to the special structure of such models, the algorithm leads to solving an algebraic equation of remarkable simplicity and physiological relevance: the type of excitability of a neuronal model is primarily determined by a balance between competitive and cooperative ion channels. The condition is also robust because the balance is independent of the detailed kinetics. It only relies on a classification of variables in three well separated time-scales, in full accordance with what is known on ion channels kinetics [8].

A same mathematical prediction applies to many distinct physiological observation

Although purely mathematical in nature, the transcritical bifurcation has a remarkable predictive value in several published conductance based models. In each of the six analysed models, the proposed algorithm identifies a physiological parameter that acts as a tuner of neuronal excitability in a physiologically plausible range and in full agreement with existing experimental data. At the same time, the distinct nature of the regulating parameter, which can be either the maximal conductance or the inactivation gating variable of a cooperative ion channel depending on the neuron model, is associated to distinctly different regulation mechanisms.

Reduced modelling should retain the balancing channel

The classification of gating variables in three distinct time scale is an essential modelling step both for the proposed algorithm and for the reduction of full conductance-based models to low-dimensional models that can be used in population studies [28]. When all recovery ion channels are properly identified, they can be aggregated in a single recovery variable to lead to a second order model of the type (1), where the single parameter n_0 captures the competitive or cooperative nature of the aggregated recovery variable. Further reduction to a one-dimensional hybrid model with reset is possible thanks to the time-scale sepration between the voltage V and the recovery variable n. This reduction is illustrated in [11] on the thalamic TC neuron and the reduced model remarkably retains the switch of excitability of its high-dimensional counterpart. In contrast, a reduced model will loose the switch of excitability of the full conductance-based model when a cooperative ion channel is treated as a fast gating variable. This is for instance the case in the STN neuron model of [29]. The switch of excitability is well identified in experimental data [30] but cannot be reproduced in the model because the only source of cooperativity, the activation of T-type calcium channels, is treated as a (instantaneous) fast variable.

Neuronal excitability is regulated

In each of the analysed conductance-based models, the balance equation responsible for the switch of excitability is satisfied in a physiological range of parameters. This observation supports the hypothesis that neuronal excitability is highly regulated by molecular mechanisms. Our experiment on the dopaminergic neuron illustrates how the density of L-type calcium channels is a key regulator of excitablity. This density could be adapted, for instance, by phosphorylation/dephosphorylation mechanisms. From a physiological point of view, a potential regulation mechanisms of DA neuron bursting through L-type calcium channel phosphorylation/dephosphorylation might rely on metabotropic receptors.

Materials and Methods

Numerical analysis

Numerical temporal traces of the different neuron models were run in MATLAB[2]. The phase portraits in Figures 1 and 3 were hand-drawn using the Open Source vector graphics editor Inkscape[3]. The phase portraits in Figure 5 were numerically drawn with MATLAB and modified with Inkscape. The bifurcation diagrams in Figures 5 and 8 were drawn by implementing the algorithm of Table 2 in MATLAB.

In vitro extracellular recordings

Housing

Adult (200-250 g) male Wistar rats were housed in groups of three or four, supplied with food and water ad libitum, and maintained on a 12 hour light/dark cycle.

Tissue preparation

Rats were anesthetized with chloral hydrate (400 mg/kg, i.p) and decapitated. The brain was extracted out of the skull in less than 1 min and cooled in ice-cold ($2 - 4$°C) artificial cerebrospinal fluid (ACSF) of the following composition (in mM): $NaCl, 130$; $KCl, 5$; $NaH_2PO_4, 1.25$; $MgSO_4, 1.25$; $CaCl_2, 2$; $D - glucose, 10$; $NaHCO_3, 24$; saturated with $95\% O_2$ and $5\% CO_2$ (pH 7.4).

Horizontal slices (400 μm) containing the midbrain were cut in cold ACSF in a vibratome and transferred to a small beaker containing ACSF at 32°C. After 10-30 min slices were transferred to the recording chamber (volume 0.5 ml) in which they were completely submerged and superfused by ACSF at a rate of 2.5 ± 0.5 ml/min (T°: 34.5 ± 0.5°C). The tissue was held in position by small platinum weights.

Action potential recordings and identification of neurons

Action potentials (amplitude: 200 to 1000 μV) were recorded extracellularly using borosilicate capillaries (model 1403516, Hilgenberg, Malsfeld, Germany) which had been pulled on a Narishige (PE-2) vertical puller. The tip resistance was 5-20 $M\Omega$. They were passed through an impedance adapter and amplified one thousand times with a home made amplifier. They were displayed on an oscilloscope and fed to an analog digital interface

---

[2] `http://www.mathworks.com`

[3] `http://inkscape.org`

(CED 1401) connected to a computer. Data were collected with the use of the ?Spike 2? software (version 4.23, Cambridge Electronic Design, Cambridge, UK). Use of an appropriate template ensured that the activity of only one cell was recorded.

Electrophysiological criteria were used in order to identify DA neurons. In vitro, these neurons exhibit a very regular firing pattern and long (≥ 2.5 ms), triphasic spikes, often displaying a prominent notch in the initial positive rising phase. They have a slow firing rate comprised between 0.5 and 5 Hz. A large number of previous experiments in our laboratory have shown that the firing of these cells is inhibited by nanomolar concentrations of D2 agonists such as quinpirole and BHT920. This was verified again in this study in the absence of synaptic blockers. Neurons meeting these criteria were selected for recording.

Only one cell was studied per slice. All recordings were made in the substantia nigra pars compacta area. Drugs were applied by superfusion at known concentrations using three-way taps. Each concentration was applied for at least 10 min to ensure that the drug concentration reached equilibrium in the tissue. Drug effects were quantified by calculating the mean firing frequency over the 5 last minutes of the control period and over the last minute during which the drug was superfused. Synaptic blockers were superfused throughout all experiments unless stated otherwise. Neurons whose firing rate varied by more than 5% (average of 1 min) during the control period were discarded.

Experimental protocol

The activity of DA neurons was recorded in control conditions for 5 minutes. Synaptic blockers (10 μM CNQX, 1 μM MK801, 10 μM SR95531, 1 μM sulpiride and 1 μM CGP55845 to block AMPA, NMDA, GABA$_A$, D2 and GABA$_B$ receptors, respectively) were then superfused for the remainder of the experiment. After at least 10 minutes, SK channels were blocked by bath application of 300 nM apamin for the remaining of the experiment. At least 10 minutes after the beginning of SK channel blockade, L-type calcium channels were blocked by bath application of 20 μM nifedipine for 10 minutes as well.

Drugs

The sources of the drugs used were as follows. CGP55845, CNQX, MK801, TTX and Nifedipine were obtained from Tocris Cookson (Bristol, UK). SR95531 and apamin was obtained from Sigma (St Louis, MO, USA). Sulpiride was a gift from Sanofi-Aventis.

Acknowledgments

References

[1] Franci A, Drion G, Sepulchre R (2012) An organizing center in a planar model of neuronal excitability. SIAM J Appl Dyn Syst (in press, preprint: `http://arxivorg/abs/12045686`) .

[2] Hodgkin A, Huxley A (1952) A quantitative description of membrane current and its application to conduction and excitation in nerve. J Physiol 117: 500-544.

[3] Drion G, Massotte L, Sepulchre R, Seutin V (2011) How modeling can reconcile apparently discrepant experimental results: The case of pacemaking in dopaminergic neurons. PLoS Comput Biol 7: e1002050.

[4] Destexhe A, Neubig M, Ulrich D, Huguenard J (1998) Dendritic low-threshold calcium currents in thalamic relay cells. J Neurosci 18: 3574–3588.

[5] Destexhe A, Contreras D, Steriade M, Sejnowski T, Huguenard J (1996) In vivo, in vitro, and computational analysis of dendritic calcium currents in thalamic reticular neurons. J Neurosci 16: 169–185.

[6] Rinzel J, Lee Y (1987) Dissection of a model for neuronal parabolic bursting. J Math Biol 25: 653–675.

[7] D'Angelo E, Nieus T, Maffei A, Armano S, Rossi P, et al. (2001) Theta-frequency bursting and resonance in cerebellar granule cells: experimental evidence and modeling of a slow K+-dependent mechanism. J Neurosci 21: 759–770.

[8] Hille B (1984) Ionic channels of excitable membranes. Sunderland, MA: Sinauer Associates Inc, 426 pp.

[9] FitzHugh R (1961) Impulses and physiological states in theoretical models of nerve membrane. Biophysical J 1: 445–466.

[10] Rinzel J (1985) Excitation dynamics: insights from simplified membrane models. In: Federation proceedings. Fed Proc, volume 44, p. 2944.

[11] Drion G, Franci A, Seutin V, Sepulchre R (2012) A novel phase portrait for neuronal excitability. PLoS ONE 7: e41806.

[12] Ermentrout G, Terman D (2010) Mathematical Foundations of Neuroscience. Interdisciplinary Applied Mathematics. Springer.

[13] Rinzel J, Ermentrout G (1989) Analysis of neural excitability and oscillations. In: Methods in neuronal modeling. MIT Press, pp. 135–169.

[14] Izhikevich E (2007) Dynamical Systems in Neuroscience: The Geometry of Excitability and Bursting. MIT Press.

[15] Thomas R (1994) The role of feedback circuits: Positive feedback circuits are a necessary condition for positive real eigenvalues of the jacobian matrix. Berichte der Bunsengesellschaft fr physikalische Chemie 98: 1148–1151.

[16] Moore J (1959) Excitation of the squid axon membrane in isosmotic potassium chloride. Nature 183: 265–266.

[17] Waroux O, Massotte L, Alleva L, Graulich A, Thomas E, et al. (2005) SK channels control the firing pattern of midbrain dopaminergic neurons in vivo. Eur J Neurosci 22: 3111–3121.

[18] Drion G, Seutin V, Sepulchre R (2012) Mitochondrion-and endoplasmic reticulum-induced SK channel dysregulation as a potential origin of the selective neurodegeneration in Parkinsons disease. Systems Biology of Parkinson's Disease : 57–79.

[19] Ji H, Hougaard C, Herrik K, Strøbæk D, Christophersen P, et al. (2009) Tuning the excitability of midbrain dopamine neurons by modulating the Ca2+ sensitivity of SK channels. Eur J Neurosci 29: 1883–1895.

[20] McCormick D, Bal T (1997) Sleep and arousal: thalamocortical mechanisms. Annual review of neuroscience 20: 185–215.

[21] Sherman S (2001) Tonic and burst firing: dual modes of thalamocortical relay. Trends Neurosci 24: 122–126.

[22] Guzman J, Sánchez-Padilla J, Chan C, Surmeier D (2009) Robust pacemaking in substantia nigra dopaminergic neurons. J Neurosci 29: 11011–11019.

[23] Putzier I, Kullmann P, Horn J, Levitan E (2009) Cav1. 3 channel voltage dependence, not Ca2+ selectivity, drives pacemaker activity and amplifies bursts in nigral dopamine neurons. J Neurosci 29: 15414–15419.

[24] Guzman J, Sanchez-Padilla J, Wokosin D, Kondapalli J, Ilijic E, et al. (2010) Oxidant stress evoked by pacemaking in dopaminergic neurons is attenuated by DJ-1. Nature 468: 696–700.

[25] Ilijic E, Guzman J, Surmeier D (2011) The L-type channel antagonist isradipine is neuroprotective in a mouse model of Parkinson's disease. Neurobiol Dis 43: 364–371.

[26] Surmeier D, Guzman J, Sanchez-Padilla J, Schumacker P (2011) The role of calcium and mitochondrial oxidant stress in the loss of substantia nigra pars compacta dopaminergic neurons in Parkinson's disease. Neuroscience 198: 221–231.

[27] Sulzer D, Surmeier D (2012) Neuronal vulnerability, pathogenesis, and Parkinson's disease. Mov Disord .

[28] Izhikevich E, Edelman G (2008) Large-scale model of mammalian thalamocortical systems. Proc Natl Acad Sci U S A 105: 3593-3598.

[29] Kubota S, Rubin J (2011) NMDA-induced burst firing in a model subthalamic nucleus neuron. J Neurol Neurophysiol 106: 527-537.

[30] Hallworth N, Wilson C, Bevan M (2003) Apamin-sensitive small conductance calcium-activated potassium channels, through their selective coupling to voltage-gated calcium channels, are critical determinants of the precision, pace, and pattern of action potential generation in rat subthalamic nucleus neurons in vitro. The Journal of neuroscience 23: 7525–7542.

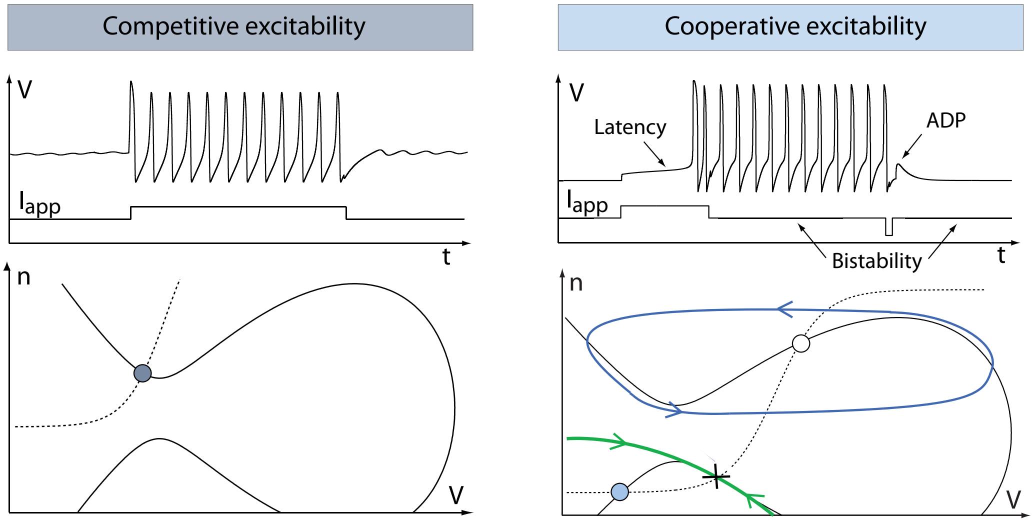

Figure 1. The bottom figures illustrate the typical phase portrait of competitive (left) and cooperative (right) excitability. The dark (resp. light) blue circle denotes a stable competitive (resp. cooperative) steady state $(\bar{V},\bar{n})$. The full (resp. dashed) line is the voltage (resp. recovery variable) nullcline. The saddle point in the right phase portrait is represented as the cross and its separatrix as the green oriented line. The stable limit cycle surrounding the unstable fixed point (represented as a circle) is represented by the blue oriented line. The top figures illustrate the typical accompanying electrophysiological responses to step variations of current.

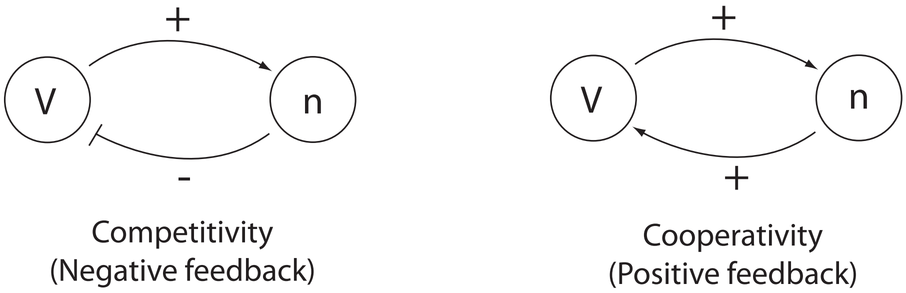

Figure 2. Block diagrams representation of competitive and cooperative excitability in planar models.

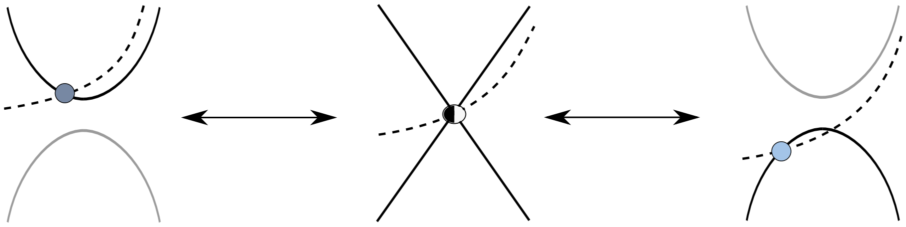

Figure 3. A continuous deformation from the competitive phase portrait of Fig. 1 left to the cooperative phase portrait of Fig. 1 right involving a transcritical bifurcation determined by the algebraic conditions (2) and (3). The dark blue circle represents a competitive stable steady-state, the light blue circle a cooperative stable steady-state, and the half-filled circle represents the transcritical bifurcation which separates the competitive and cooperative regimes.

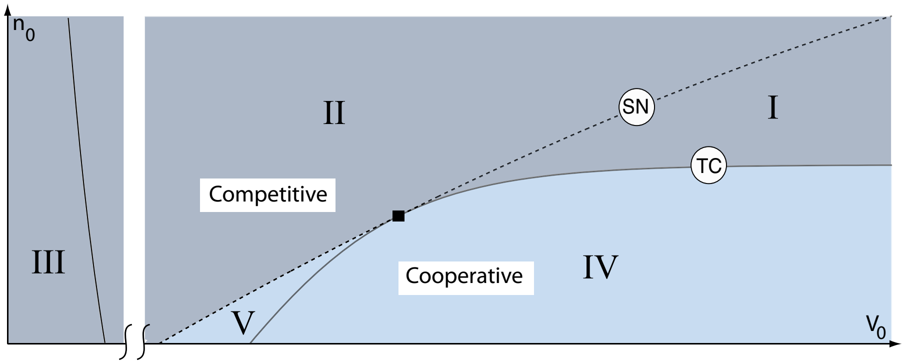

Figure 4. Excitability types in model (1). SN denotes the saddle-node bifurcation, TC the transcritical bifurcation. ■: Pitchfork bifurcation organizing center. Varying n_0 and V_0 the model switches between excitability types.

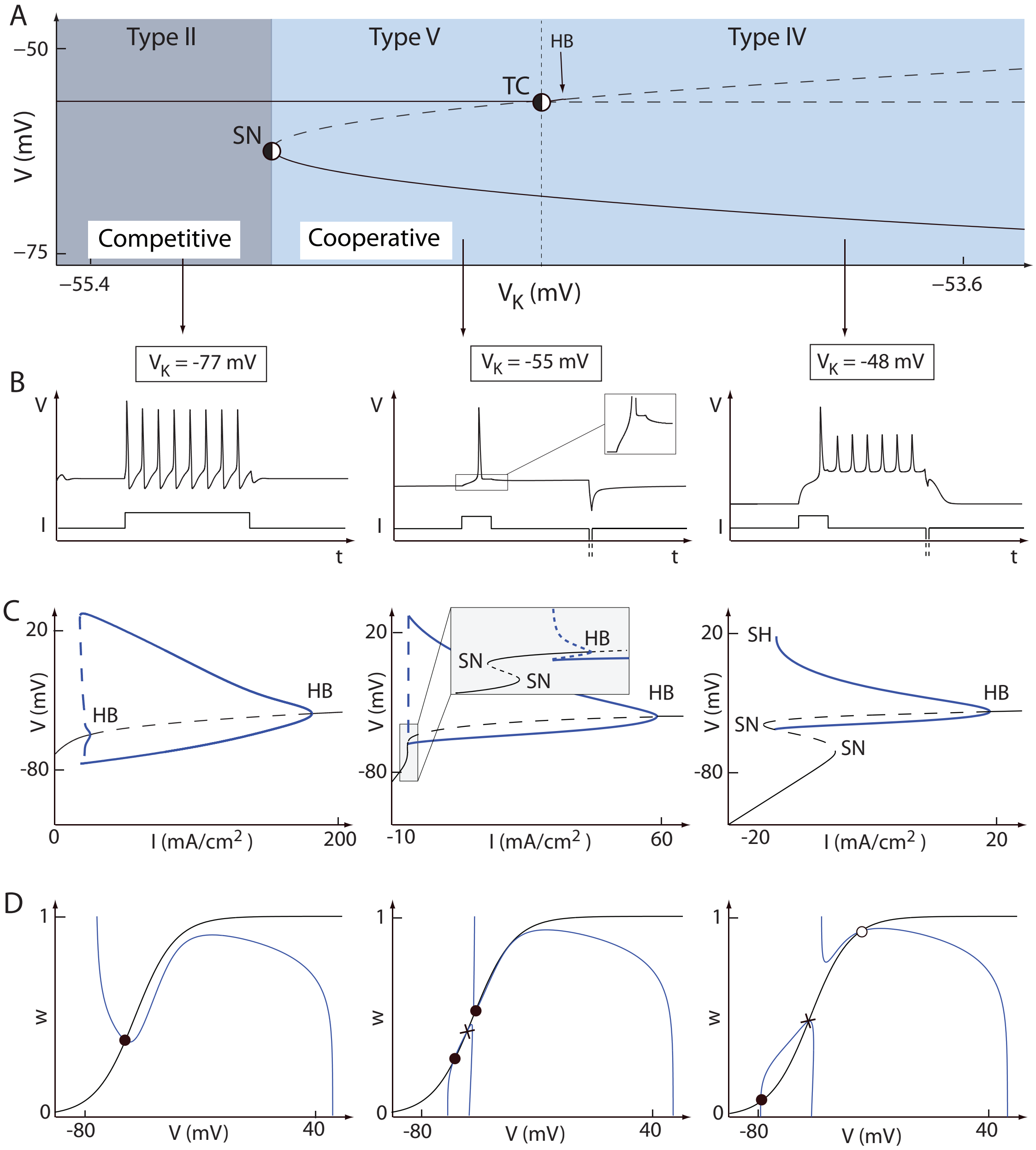

Figure 5. Variations of the potassium reversal potential V_K induce excitability switches in the Hodgkin-Huxley model. **A.** Bifurcation diagram of the HH model with V_K as the bifurcation parameter. TC denotes a transcritical bifurcation, SN a saddle-node bifurcation, HB a Hopf bifurcation. Branches of stable fixed points are represented as solid line, whereas branches of saddle points and unstable points as dashed lines. **B.** Electrophysiological responses of the model for three different values of V_K, corresponding to three different excitability types (Type I, V and IV, from left to right). **C.** Bifurcation diagrams with the applied current as the bifurcation parameter for the same three values of V_K as in **B**. Black (resp. blue) full lines represent branches of stable steady-states (resp. limit cycles), black dashed lines branches of saddle and unstable steady-states. Branches of unstable limit cycle are drawn as dashed blue lines. HB denotes a Hopf bifurcation, SN a saddle-node bifurcation, and SH a saddle-homoclinic bifurcation. **D.** Phase portraits of reduced HH model proposed by Rinzel in [10] for the same three values of V_K as in **B,C**. Blue full lines denote the V-nullclines and black full lines the w-nullclines, where w denotes the recovery variable of the reduced model. Filled circles denote stable steady-states, crosses saddle points, and circles unstable steady-states.

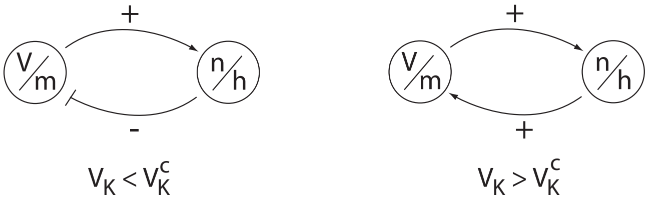

Figure 6. Representation of HH model excitability as feedback interconnections. The membrane potential V and the sodium channel activation m are the fast variables, the potassium channel activation n and the sodium channel inactivation h are the slow recovery variables. When V_K is below (resp. above) the critical value V_K^c, recovery variables induce an overall negative (resp. positive) feedback on membrane potential variations, resulting in competitive (resp. cooperative) excitability.

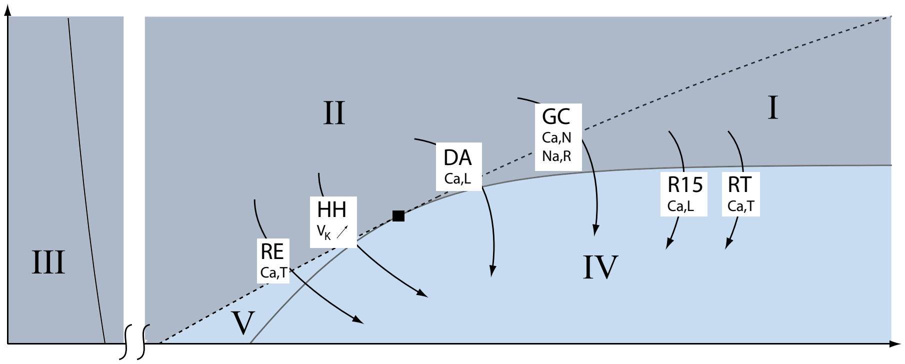

Figure 7. Modifications in the balance between competitive and cooperative channels induce excitability switches in conductance-based models. The figure sketches excitability switches of the Hodgkin-Huxley (HH) model [2], Aplysia's R15 neuron (R15) model [6], a dopaminergic (DA) neuron model [3], thalamic reticular (RT) and relay (RE) neuron models [4, 5], and a cerebral granule cell (GC) model [7] on the excitability parameter map computed for the two-dimensional model of [1]. All these conductance-based models can switch between competitive and cooperative excitability through the physiologically relevant regulation of specific ion channels.

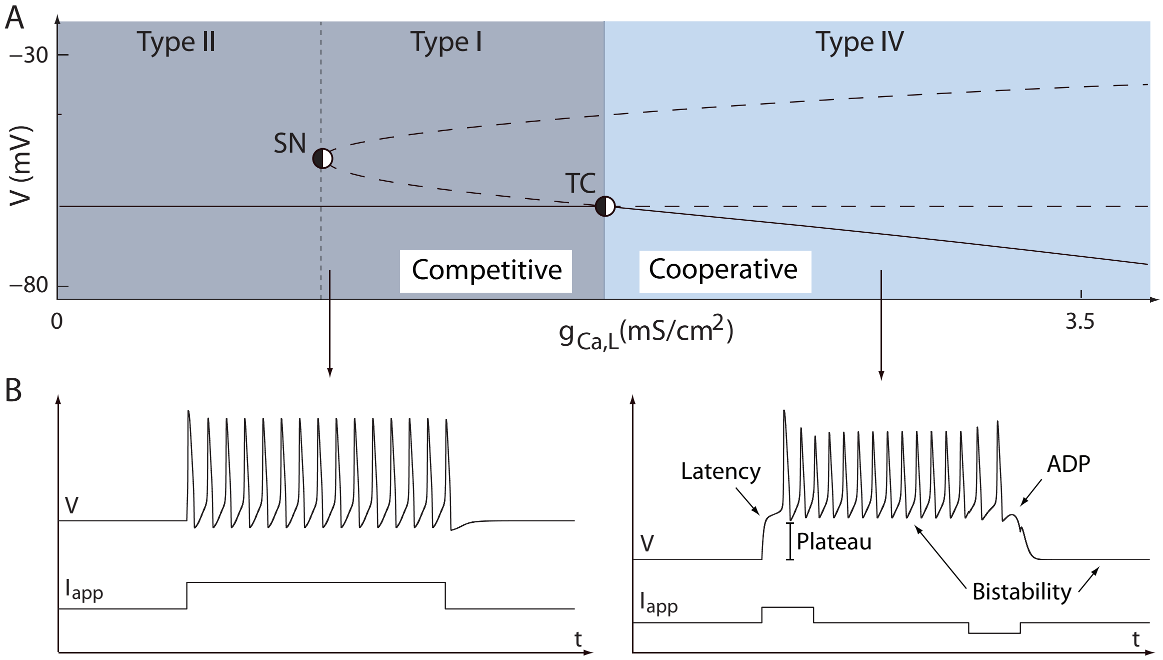

Figure 8. Variations of L-type calcium channel density $\bar{g}_{Ca,L}$ induces excitability switches in a model of DA neurons [3]. A. Bifurcation diagram of the model with $\bar{g}_{Ca,L}$ as the bifurcation parameter. TC denotes a transcritical bifurcation, SN a saddle-node bifurcation. Branches of stable fixed points are represented as solid line, branches of saddle points and unstable points as dashed lines. **B.** Electrophysiological responses of the model to step inputs of excitatory/inhibitory current (the intracellular calcium concentration is fixed at $[Ca^{2+}]_{in} = 300\,nM$, which is within the physiological range). For $\bar{g}_{Ca,L}$ lower (resp. higher) than the critical value $\bar{g}^c_{Ca,L}$, the model exhibits typical electrophysiological signature of competitive (resp. cooperative) excitability. The low $\bar{g}_{Ca,L}$ configuration corresponds to $\bar{g}_{Ca,L} = 1mS/cm^2$, whereas the high $\bar{g}_{Ca,L}$ configuration corresponds to $\bar{g}_{Ca,L} = 3mS/cm^2$.

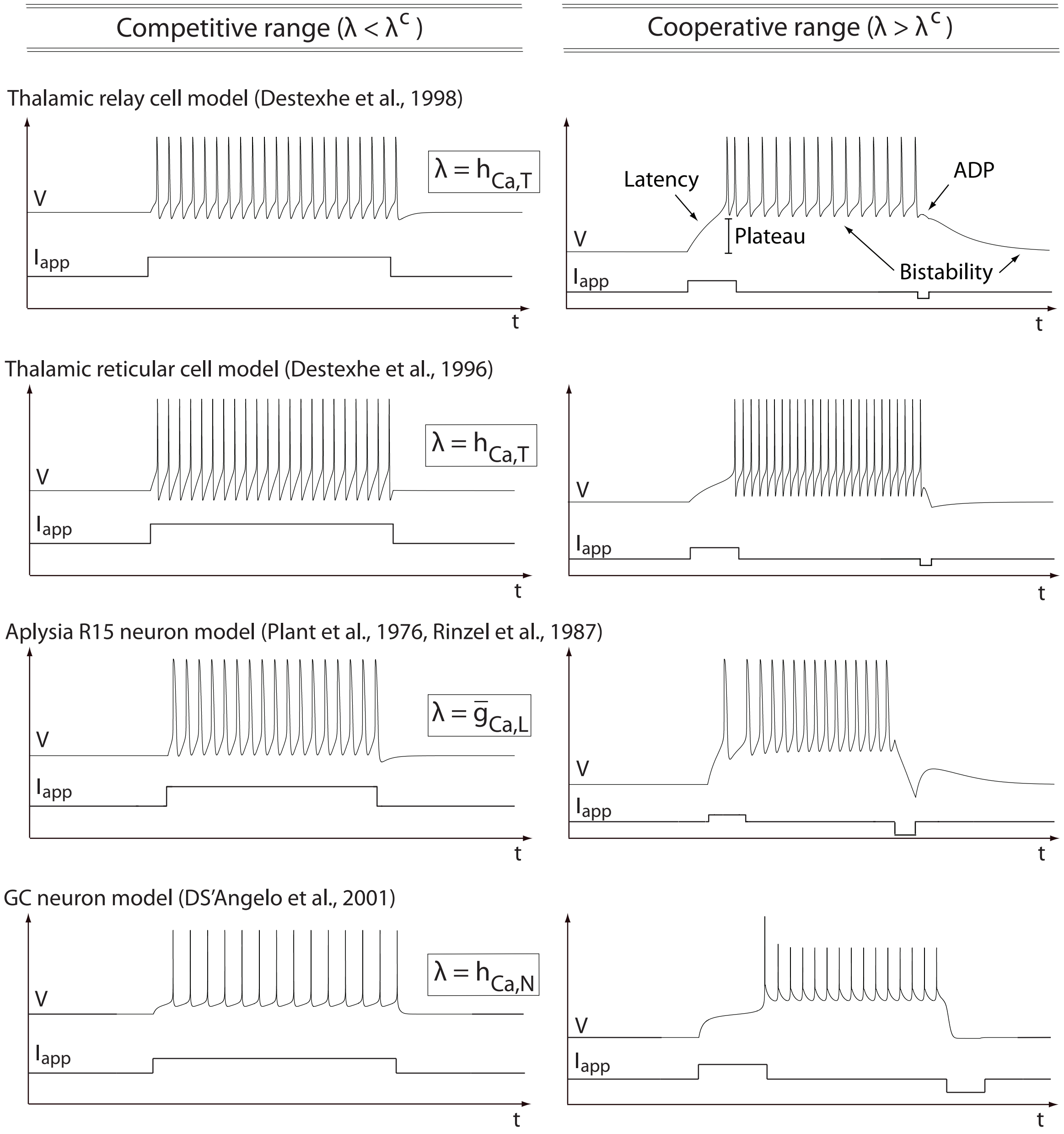

Figure 9. The same mathematical bifurcation in different conductance-base models causes the same switch in electrophysiological signatures. The figure shows the electrophysiological responses of various conductance-based models to step inputs of excitatory/inhibitory current when the bifurcation parameter λ is lower (left) or higher (right) than the critical value λ^c. This bifurcation parameter can be either the density or the inactivation variable of a cooperative channel. Other adaptation variables are set to constant values chosen in physiological ranges (see text). For λ lower (resp. higher) than the critical value λ^c, all models exhibit electrophysiological signatures of competitive (resp. cooperative) excitability. Numerical values of the parameter λ in the different plots are as follows. Thalamic relay cell: left $h_{Ca,T} = 0$, right $h_{Ca,T} = 0.2$. Thalamic reticular cell: left $h_{Ca,T} = 0$, right $h_{Ca,T} = 0.4$. Aplysia R15 neuron: left $\bar{g}_{Ca,L} = 10^{-6} mS/cm^2$, right $\bar{g}_{Ca,L} = 0.004 mS/cm^2$. GC neuron: left $h_{Ca,N} = 0$, right $h_{Ca,N} = 0.3$.

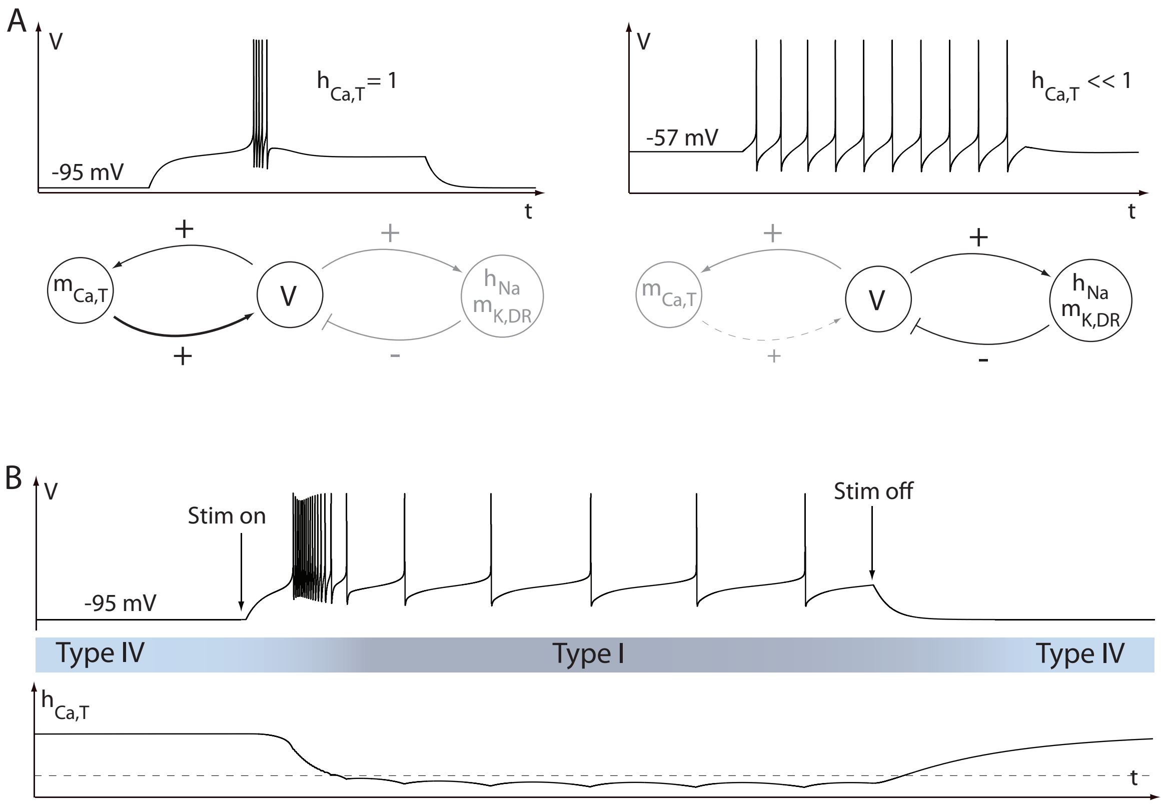

Figure 10. Thalamocortical reticular and relay cell signaling relies on dynamical switches between competitive and cooperative excitability, through the regulation of T-type calcium channel inactivation. A. Electrophysiological responses of a full TC reticular cell model [5] to a step input of excitatory current starting from a hyperpolarized (left) or depolarized (right) steady-state. An initial hyperpolarization of the cell releases T-type calcium channel inactivation, inducing a switch from competitive to cooperative excitability responsible for the two distinctly different electrophysiological responses. Feedback interconnections illustrate the switch between competitive and cooperative excitability induced by the regulation of T-type calcium channel inactivation (the darker the arrows, the stronger the feedback loop). **B.** Electrophysiological responses of the same TC reticular cell model to a step input of excitatory current of higher amplitude, starting from a hyperpolarized resting state. The figure shows variations of membrane potential (top) and T-type calcium channel inactivation (bottom) over time. The neuron dynamically switches from cooperative to competitive excitability during the excitation, due to T-type calcium channel inactivation. This results in the generation of a transient burst followed by low-frequency single-spike firing.

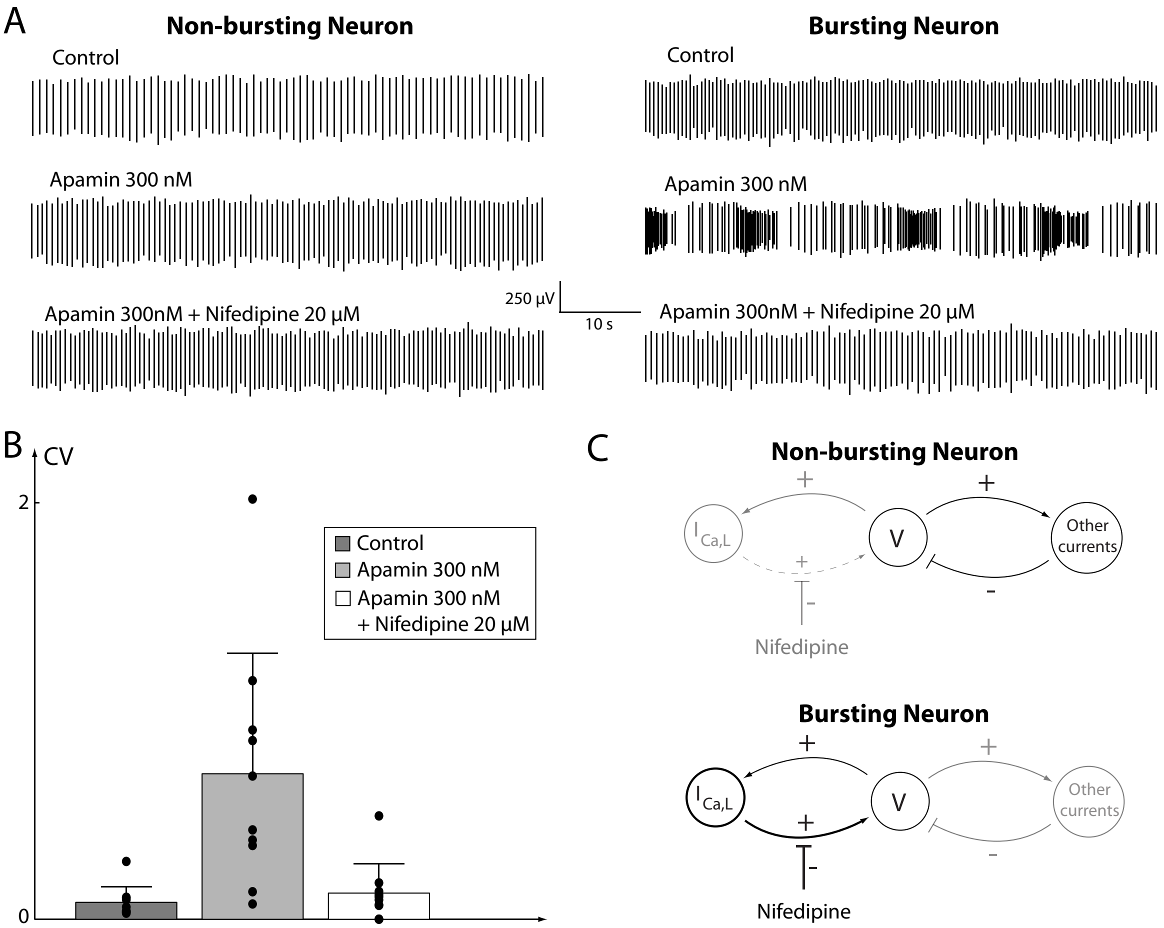

Figure 11. The heterogeneity of dopaminergic (DA) neuron L-type calcium channel density is responsible for an heterogeneity in their firing pattern. A. Extracellular recordings of substantia nigra of two DA neurons from rat brain slices in control condition (top), during SK channel blockade (middle), and during concomitant blockade of SK channel and L-type calcium channel (bottom). **B.** Coefficient of variations of neuron firing patterns in each condition. Black point represents values for each neuron, bars represents the mean values and the standard deviation. **C.** Feedback interconnections illustrating the heterogeneity in DA neuron firing pattern after SK channel blockade and in the effect of the L-type channel blocker nifedipine (the darker the arrow, the stronger the feedback). Although DA neurons exhibit similar firing patterns in control conditions, SK channel blockade uncovers an heterogeneity, some DA neuron exhibiting electrophysiological signature of competitive excitability, namely single-spike firing, others of cooperative excitability, namely burst firing. A L-type calcium channel blockade solely affect the firing pattern of bursting neurons, inducing a switch from cooperative to competitive excitability, as predicted above.

Supplementary material

Construction of the transcritical bifurcation in generic conductance-based models

Suppose that, given a bifurcation parameter $\mu \in \{\bar{g}_i, E_i\}_{i\in\mathcal{I}}$, there exists a a solution $(V,\mu) = (V_{TC}, \mu_{TC})$ satisfying the two degeneracy conditions (7) and (8). Then we claim that, posing

$$I_{TC} = \sum_i \bar{g}_i m_{i\infty}^{a_i}(V_{TC}) h_{i\infty}^{b_i}(V_{TC})(V_{TC} - E_i),$$

which solves the fixed point equation, the model is at a transcritical bifurcation. The existence of the couple (V_{TC}, μ_{TC}) in the physiological range is shown for specific examples in the main document.

The center space E_c associated to the degeneracy conditions (7) and (8) is spanned by the vector

$$v_c = (1, \mathbf{k}), \quad \mathbf{k} := [k_x]_x, \quad k_x := \left.\frac{\partial x_\infty}{\partial V}\right|_{V=V_{TC}},$$

where x runs all fast and recover gating variables in the model, that is $\mathbf{k}$ is the vector whose elements are the slopes of the (in)activation functions of all the fast and recovery gating variables calculated at $V = V_{TC}$. The associated center manifold $\mathcal{M}_c$ is exponentially attractive. Indeed, it can easily been shown that, when (7) and (8) are satisfied, the remaining nonzero eigenvalues of the Jacobian of (10) are all negative. To the first order, the dynamics on $\mathcal{M}_c$ is given by

$$C_m \dot{V}_c = -\sum_{i\in\mathcal{I}} \bar{g}_i \big(m_{i,\infty}(V_{TC}) + k_{m_i}(V_c - V_{TC})\big)^{a_i} \big(h_{i,\infty}(V_{TC}) + k_{h_i}(V_c - V_{TC})\big)^{b_i} (V_c - E_i) + I_{app}$$

Consider the affine reparametrization

$$\tilde{\mu} = \mu, \quad \tilde{I}_{app} = I_{app} + \left.\frac{\partial \dot{V}_c}{\partial \mu}\right|_{\substack{\mu=\mu_{TC}\\ V=V_{TC}}} (\mu - \mu_{TC}). \tag{S16}$$

It is easy to show that, in the affine reparametrization (S16), the center manifold dynamics satisfy

$$\dot{V}_c = \left.\frac{\partial \dot{V}_c}{\partial V}\right|_{\substack{\mu=\mu_{TC}\\ V=V_{TC}}} = \left.\frac{\partial \dot{V}_c}{\partial \tilde{\mu}}\right|_{\substack{\mu=\mu_{TC}\\ V=V_{TC}}} = 0$$

corresponding to the defining condition of a transcritical bifurcation (see [1, Page 367]).

Supplementary references

[1] Seydel R (2010) Practical bifurcation and stability analysis, volume 5 of *Interdisciplinary Applied Mathematics*. New York: Springer-Verlag, third edition.